

DOI: 10.5586/asbp.3530

Publication history

Received: 2016-12-05

Accepted: 2016-12-23

Published: 2016-12-31

Handling editors

Beata Zagórska-Marek, Faculty of Biological Sciences, University of Wrocław, Poland
Przemysław Prusinkiewicz, Faculty of Science, University of Calgary, Canada

Authors' contributions

MSK and KF designed research, conducted experiments, and wrote manuscript

Funding

KF is supported by a Grant-in-Aid for Scientific Research on Innovative Areas (16H01241), MEXT, Japan.

Competing interests

No competing interests have been declared.

Copyright notice

© The Author(s) 2016. This is an Open Access article distributed under the terms of the [Creative Commons Attribution License](#), which permits redistribution, commercial and non-commercial, provided that the article is properly cited.

Citation

Kitazawa MS, Fujimoto K. Stochastic occurrence of trimery from pentamery in floral phyllotaxis of *Anemone* (Ranunculaceae). *Acta Soc Bot Pol.* 2016;85(4):3530. <https://doi.org/10.5586/asbp.3530>

Digital signature

This PDF has been certified using digital signature with a trusted timestamp to assure its origin and integrity. A verification trust dialog appears on the PDF document when it is opened in a compatible PDF reader. Certificate properties provide further details such as certification time and a signing reason in case any alterations made to the final content. If the certificate is missing or invalid it is recommended to verify the article on the journal website.

INVITED ORIGINAL RESEARCH PAPER

Stochastic occurrence of trimery from pentamery in floral phyllotaxis of *Anemone* (Ranunculaceae)

Miho S. Kitazawa^{1,2}, Koichi Fujimoto^{2*}

¹ Center for Education in Liberal Arts and Sciences, Osaka University, 1-16 Machikaneyamacho, Toyonaka, Osaka, 560-0043, Japan

² Department of Biological Sciences, Osaka University, 1-1 Machikaneyamacho, Toyonaka, Osaka, 560-0043, Japan

* Corresponding author. Email: fujimoto@bio.sci.osaka-u.ac.jp

Abstract

Merosity, indicating the basic number of floral organs such as sepals and petals, has been constrained to specific and stable numbers during the evolution of angiosperms. The ancestral flower is considered to have a spiral arrangement of perianth organs, as in phyllotaxis, the arrangement of leaves. How has the ancestral spiral evolved into flowers with specific merosities? To address this question, we studied perianth organ arrangement in the *Anemone* genus of the basal eudicot family Ranunculaceae, because various merosities are found in this genus. In three species, *A. flaccida*, *A. scabiosa*, and *A. nikoensis* that are normally pentamerous, we found positional arrangement of the excessive sixth perianth organ indicating the possibility of a transition from pentamerous to trimerous arrangement. Arrangement was intraspecifically stochastic, but constrained to three of five types, where trimerous arrangement was the most frequent in all species except for a form of *A. scabiosa*. The rank of frequency of the other two types was species-dependent. We connect these observations with classical theories of spiral phyllotaxis. The phyllotaxis model for initiation of the sixth organ showed that the three arrangements occur at a divergence angle $<144^\circ$, indicating the spiral nature of floral phyllotaxis rather than a perfect penta-radial symmetry of 144° . The model further showed that selective occurrence of trimerous arrangement is mainly regulated by the organ growth rate. Differential organ growth as well as divergence angle may regulate transitions between pentamerous and trimerous flowers in intraspecific variation as well as in species evolution.

Keywords

phenotypic variation; phyllotaxis; perianth; whorl; merosity; floral organ; Ranunculaceae; *Anemone*

Introduction

The basic number of floral organs (e.g., sepals and petals), known as merosity, has been constrained to specific and stable numbers during angiosperm evolution. Most eudicots have multiples of five or four floral organs in pentamerous or tetramerous whorls, meaning that the organs are arranged in concentric circles (Fig. 1a), whereas most monocots and Magnoliids have merosities of three (Fig. 1b). Referring to spiral flowers of basal angiosperms (e.g., Amborellales and Austrobaileyales) [1], ancestral flowers are considered to have spirally arranged perianth organs, similar to spiral phyllotaxis. From the ancestral state with an unspecified number of perianth organs, how have flowers evolved whorls with specific merosities? While phyllotaxis studies have shown that transitions between spiral and whorled arrangements (Fig. 1a,b) can be caused by the size or growth speed of meristem [2,3], little is known about developmental mechanisms that determine the specific number of perianth organs. We

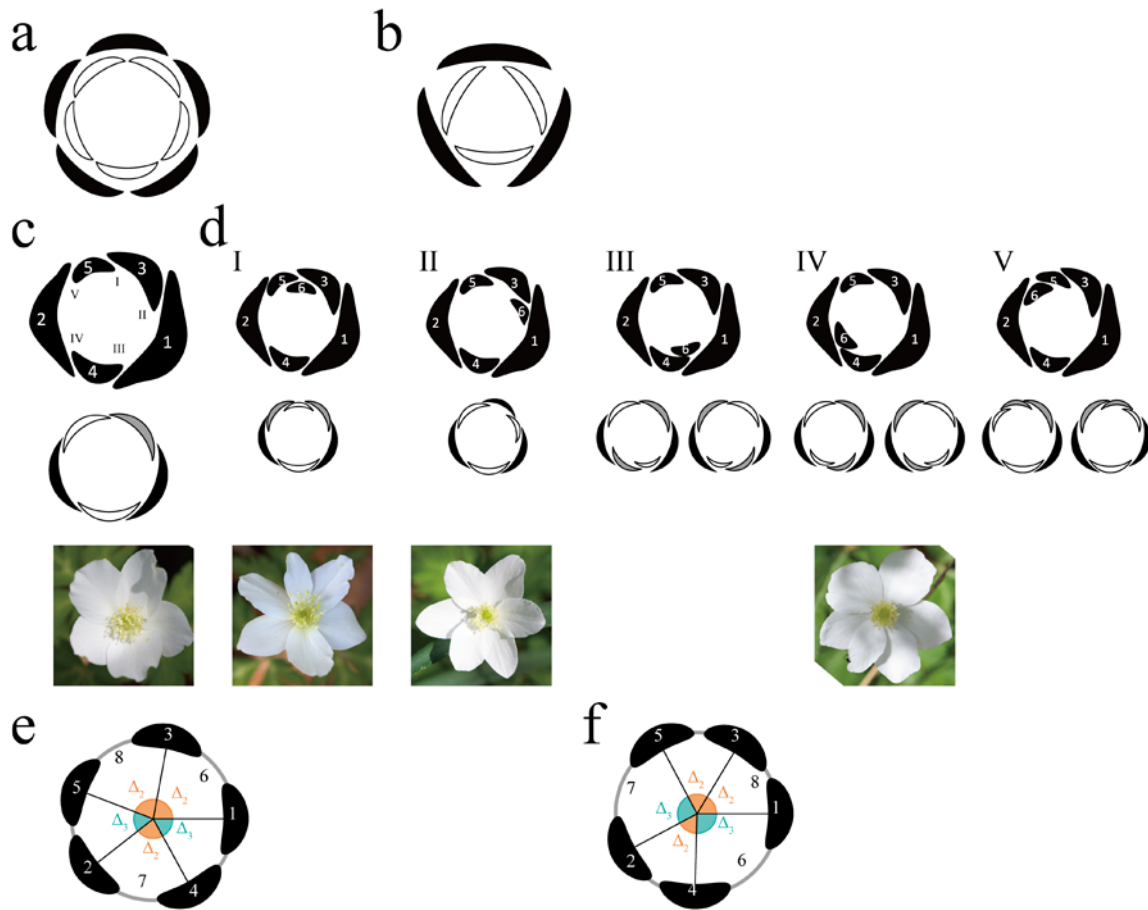


Fig. 1 Schematic diagram of evolutionary development of floral organ numbers. **a,b** Concentric organ arrangement of pentamerous (**a**) and trimerous (**b**) flowers. **c** Spiral arrangement with temporal order of organ initiation denoted by Arabic numerals, while Roman numerals denote five possible positions of an excessive tepal (top). Corresponding overlapping patterns of tepals in mature flowers (middle) and a representative example of *A. nikoensis* (bottom). **d** Five possible initiation patterns (top), corresponding overlapping patterns of tepals in mature flowers (middle). Reflected arrangement can be distinguished for V–III, but we counted them together in this paper. Organs in bottom panels of **c** and **d** are categorized by positional arrangement with neighboring organs: external (black) and internal (open) indicate that both sides of the organ are external and internal, respectively, to the neighboring organs. The alternating (grey) denotes that either of the organ sides is external and the other is internal to the neighboring organs. Examples of *A. nikoensis* (**c** and **d**, bottom) were observed within a population (Okayama2 in Fig. 3). **e** and **f** show the schematic diagram of the spiral arrangement of five organs with angular vacancies Δ_2 and Δ_3 (Eq. 2). 6, 7, and 8 denote initiation position of subsequent organs. Divergence angle $\varphi = 140^\circ$ (**e**; Eq. 1), $\varphi = 150^\circ$ (**f**).

previously improved phyllotaxis models by showing that tetramerous and pentamerous whorls emerge from spiral initiation of floral organ primordia, as observed in eudicot flower development, and that whorl emergence depends on the rate of organ growth independent of meristem properties [4]. Transitions between pentamerous and trimerous whorls (Fig. 1a,b), however, remain elusive.

To better understand the transitions between pentamerous and trimerous whorls, the genus *Anemone* in the family Ranunculaceae is promising because of the interspecific diversity of merosity within the genus. The perianths of *Anemone* flowers consist of several perianth organs without distinction between calyx and corolla, whose numbers differ among species. Based on phylogeny of the genus *Anemone* [5], the tepal (perianth organ) numbers of their flowers have experienced multiple changes. There are two types of perianth arrangement: pentamerous single-perianth (Fig. 1c, top panel) and trimerous double-perianth (Fig. 1d, II – top panel), respectively. The former shows spiral initiation similar to sepal development in core eudicots [6], while the latter arrangement is similar to monocots.

Anemone flowers frequently have intraspecific variation in tepal numbers within populations, as seen in many angiosperm clades [7,8]. For example, variation in *A. flaccida* indicated that the basic (i.e., most stable) number of tepals is five, whereas

that in some populations of species such as *A. scabiosa* and *A. nikoensis* imply that it is six [9]. This deviation may indicate that the basic number of floral organs is shifted from five to six, implying a relationship to trimery, since these species stochastically show flowers with six tepals, including the trimerous arrangement (II in Fig. 1d). Moreover, the intermediate initiation of spiral and trimerous patterns was observed in the genus [6]. Hence, variation of *Anemone* flowers may reflect the transient state of spiral phyllotaxis to a stable arrangement, including both three and five, in a fixed number of organs. This possibility prompted us to explore conditions for transition between trimerous and pentamerous whorls.

In this paper, using three species of *Anemone*, *A. flaccida*, *A. scabiosa*, and *A. nikoensis*, each with a modal number of five perianth organs, we recorded the arrangement of perianth organs focusing on the position of the sixth perianth organ in mature flowers. As in phyllotaxis [10], a new primordium arises within a vacancy between two earlier primordia during *Anemone* floral development [6], thus, there are five possible positions of the sixth tepal (Fig. 1d). Among these possibilities, only three positions, including trimerous whorls, selectively occurred with a biased frequency depending on form or species. These three positions were consistent with a continuous spiral having a constant divergence angle in the phyllotaxis. The model further suggests that the organ growth rate, which plays a central role in the transition between tetramerous and pentamerous whorls [4], also has a central role in biasing the frequency of trimerous whorls.

Material and methods

Positional arrangement of perianth organs

The arrangement of tepals in *Anemone* flowers with five tepals is stably quincuncial (Fig. 1c), consistent with earlier observations of *Ranunculus* (Ranunculaceae) calyx [11]. The sepal initiation order of *Ranunculus* is the spiral [12] (Fig. 1c, top), suggesting that the initiation pattern to be conserved in the blooming flowers. Therefore, we examined the tepal arrangement of mature flowers to trace their developmental process. Based on observations of stamen primordia initiation following formation of tepals [6], the sixth tepal should be arranged between a pair of neighboring, pre-existing tepals. Thus, there are five potential sites for tepal initiation (Fig. 1d). We counted the frequencies of five possible tepal arrangements in wild populations of four *Anemone* species, focusing only on flowers with six tepals. These five types were distinguished from mature flowers by identifying the arrangement of each organ relative to neighboring organs, either external, internal, or alternating (Fig. 1d, middle and bottom). For simplicity, reflected (Fig. 1d, III–V middle) and rotated arrangements were not distinguished. Specifically, whether the spiral direction was CW or CCW did not affect the results. We paid special attention to the frequency of Type II arrangements that had the same overlapping pattern as trimerous whorls.

Plant samples

Our study mainly used Japanese anemone (known as *A. hupehensis* var. *japonica*; *Anemone scabiosa* according to The Plant List, <http://www.theplantlist.org>; last access: November 17, 2016). There are several forms of *A. scabiosa*, but we could not identify the forms at many of our observation sites. Therefore, we used tepal color as the primary feature to define the forms. Using tepal color, we could clearly distinguish between three groups: deep pink, pale pink, and white. Populations with deep pink tepals are further classified into a type with broad, obovate tepals, and one with thin, linear tepals, both of which were excluded from our study as the populations with broad tepals deviate little from pentamery and those with thin tepals have numerous tepals (more than 10). Thus, we only examined the pale pink and white groups. We present data on 57 pale pink and 19 white populations located within five prefectures in Japan (four in Kinki area, one in Kanto area), measured in September and October

2016. We also examined three additional *Anemone* species, *A. nikoensis*, *A. flaccida*, and *A. hepatica* var. *japonica*. *Anemone scabiosa* is a domestic species, whereas the other three are wild species endemic to Japan (*A. nikoensis* and *A. hepatica* var. *japonica*) or to East Asia (*A. flaccida*). *Anemone flaccida* was examined at the same location, in two different years. *Anemone nikoensis* was examined at four different locations, in the same year.

Phyllotaxis model – angular vacancy available for sixth organ initiation

We theoretically consider a simple situation that the tepal primordia arise as a consequence of regular spiral phyllotaxis. Suppose that five tepals are arranged in a spiral with a fixed divergence angle φ , the angular positions of the n -th tepal is:

$$\theta_n = n\varphi \bmod 360^\circ; n = 1, 2, 3, 4, 5 \quad \text{Eq. 1}$$

Quincuncial arrangement (Fig. 1c) is obtained only when $120^\circ < \varphi < 180^\circ$. When φ is smaller than 144° , the position of the sixth primordium is between the first and third primordia, i.e., Position II (Fig. 1d). Positions I and IV, are the positions of the following seventh and eighth primordia, respectively (Fig. 1e). Therefore, in spiral phyllotaxis, the positions of the sixth organ in Types I, II, and IV correspond to the positions of the sixth, seventh, and eighth primordia, respectively. In typical *Anemone* floral development, the tepal and following stamen primordia arise in a continuous spiral pattern [6], indicating that primordia appearing at the sixth-to-eighth positions stochastically become tepals rather than stamens as in typical flowers. Extension of the ABC model may explain the stochastic change of organ fate from tepal to stamen [8,13,14]. According to the ABC model, primordia consisting of a whorl obey the same organ fate (e.g., black organs in Fig. 1a,c) [15]. Therefore, if a primordium that arises after the fifth penetrates into the outer whorl, e.g., between outer primordia that are destined to be tepals, the penetrated primordium is more likely to be a tepal than a stamen.

The chance of penetration depends on the space between two organs, in an angular direction (Fig. 1e,f). By subtracting each angular position, we obtain angular vacancies for five possible positions of the sixth organ (CW direction in Fig. 1e,f):

$$\begin{aligned} \text{I: } & \theta_3 - \theta_5 = -2\varphi \bmod 360^\circ \equiv \Delta_2 \\ \text{II: } & \theta_1 - \theta_3 = -2\varphi \bmod 360^\circ = \Delta_2 \\ \text{III: } & \theta_4 - \theta_1 = 3\varphi \bmod 360^\circ \equiv \Delta_3 \\ \text{IV: } & \theta_2 - \theta_4 = -2\varphi \bmod 360^\circ = \Delta_2 \\ \text{V: } & \theta_5 - \theta_2 = 3\varphi \bmod 360^\circ = \Delta_3 \end{aligned} \quad \text{Eq. 2}$$

Angular vacancies (Eq. 2) for Types I, II, and IV equal Δ_2 while those for III and V equal Δ_3 . Thus, all five vacancies are the same ($\Delta_2 = \Delta_3$) when the organs are arranged in a regular pentagon ($\varphi = 144^\circ$), $\Delta_2 > \Delta_3$ when $\varphi < 144^\circ$ (Fig. 1e), and $\Delta_2 < \Delta_3$ when $\varphi > 144^\circ$ (Fig. 1f).

Potential function incorporating growth of primordia

We mathematically evaluated angular vacancy using “potential”, which represents the strength of inhibiting the initiation of a new primordium. Based on the observations of primordia initiation at the least crowded space, many phyllotaxis theories assume that existing organ primordia inhibit the initiation of subsequent primordia [10], and that this inhibition was formulated by an energy function [16]. As energy decreases, the chance of a new primordium emerging increases. For example, *Arabidopsis* inflorescence phyllotaxis has several local energy minima, in addition to the global minimum at divergence angle φ , which is considered to be the cause of stochasticity in angular organs positions [17,18]. For simplicity, we assume that the five organs are already arranged in a whorl with equal divergence angle φ (Eq. 1) and constant distance from the floral center R_0 (Fig. 1e,f). Each organ suppresses formation of the sixth primordium by a spatial-decaying potential energy

$$E(d_{6n}) = \sum_{n=1}^5 \exp(\alpha n) \exp\left(-\frac{d_{6n}}{\lambda}\right) \quad \text{Eq. 3}$$

as a function of d_{6n} , distance between sixth primordium and an organ n ($1 \leq n \leq 5$), where λ is the spatial-decay length. The ratio λ / R_0 is a central parameter in phyllotaxis (i.e., Γ in [2]). Following the earlier model for floral phyllotaxis, α represents the difference of inhibitory effect due to growth progression on pre-existing organs. The α can account for the change of the direction of auxin flux toward the inner tissue of primordia and/or primordial boundary establishment and the increase of primordial volume [4]. A position at the global energy minimum is expected to be the most frequently observed position, while a position at the local minima will correspond to the second or lower frequency ranks.

Results

Positional arrangement of the sixth excessive tepal of pentamerous *Anemone* species were stochastic and constrained

First, we observed four populations of *A. hepatica* consisting of 119 flowers, 59 of which had six tepals. In three populations the most frequent tepal number was six, and in one population it was eight. All flowers with six tepals showed only a Type II arrangement pattern (Fig. 1d), demonstrating that the trimerous arrangement is representative of *Anemone* flowers having six tepals as their mode.

Tepal numbers in *A. scabiosa* were highly variable, where the fraction of flowers with six tepals was 22% in the white group, and 23% in pale pink group. The most frequent tepal number was seven in the white group and five in the pale pink group, though the mode ranged from 5 to 10 depending on the population. All flowers with five tepals shows only quincuncial arrangement (Fig. 1c), confirming that it is the representative arrangement of pentamerous flower in *Anemone*. In *A. scabiosa* with six tepals, the observed arrangements were constrained to three arrangement types (I, II, and IV) of the five possible types, with Types III and V having absolute frequencies of zero (Fig. 2). Among the three observed arrangements, the relative frequency of Type I was lowest, up to 3% in both white and pale pink groups. Differences between the white and pale pink groups were observed in their relative frequencies of Types II and IV arrangements. In the group with pale pink tepals, the Type IV arrangement was found with the highest frequency, whereas the trimerous arrangement (Type II) was found most frequently in the group with white tepals (Fig. 2). Among pale pink populations containing more than 30 flowers, Type IV was more frequent than Type II in each of the five populations. In contrast, in the white group higher frequency of Type IV than Type II appeared in only two of the 12 populations.

To determine whether this frequency is common among *Anemone* species, we next examined the sixth tepal position in two additional species, *A. flaccida* and *A. nikoensis*. Similar to *A. scabiosa*, Types I, II, and IV were found at higher frequencies than the other two types. Moreover, the frequency rank of three types (i.e., II, IV, I in ascending order) in two of the four *A. nikoensis* populations was consistent with that of *A. scabiosa* white group (Fig. 3, Hyogo1 and Okayama1), while that of another population of *A. nikoensis* (i.e., IV, II, I) was consistent with *A. scabiosa* pale pink group (Fig. 3, Okayama2). In contrast to *A. scabiosa*, however, Type I had a higher relative frequency than Type IV in the other population of *A. nikoensis* and in each of the two *A. flaccida* populations (Fig. 3). Therefore, while selective appearance of Types I, II, and IV was common in three *Anemone* species, the relative magnitude of these three types was species-specific.

Inference of divergence angle by phyllotaxis model

We theoretically examined whether the constrained occurrence among arrangement Types I, II, and IV can be explained by a spiral phyllotaxis model (Eq. 1). The fact that all *A. hepatica* have Type II arrangement indicates that *A. hepatica* flowers strictly

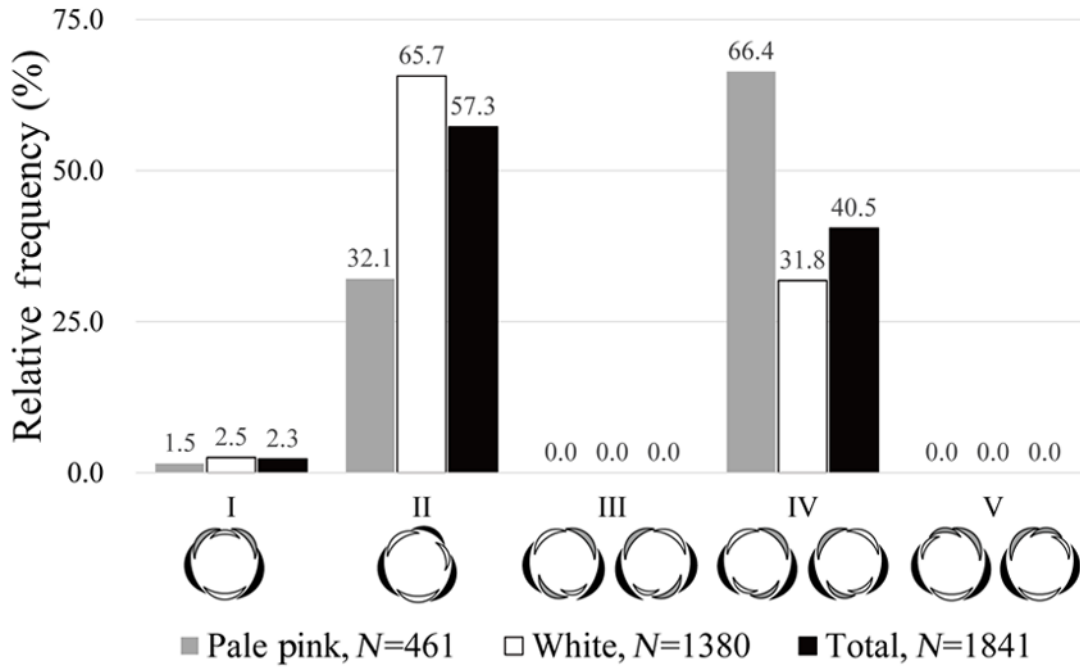


Fig. 2 Occurrence of tepal arrangements measured for flowers with six tepals in *Anemone scabiosa* populations. Chart shows the total of 57 (pale pink) and 19 (white) populations.

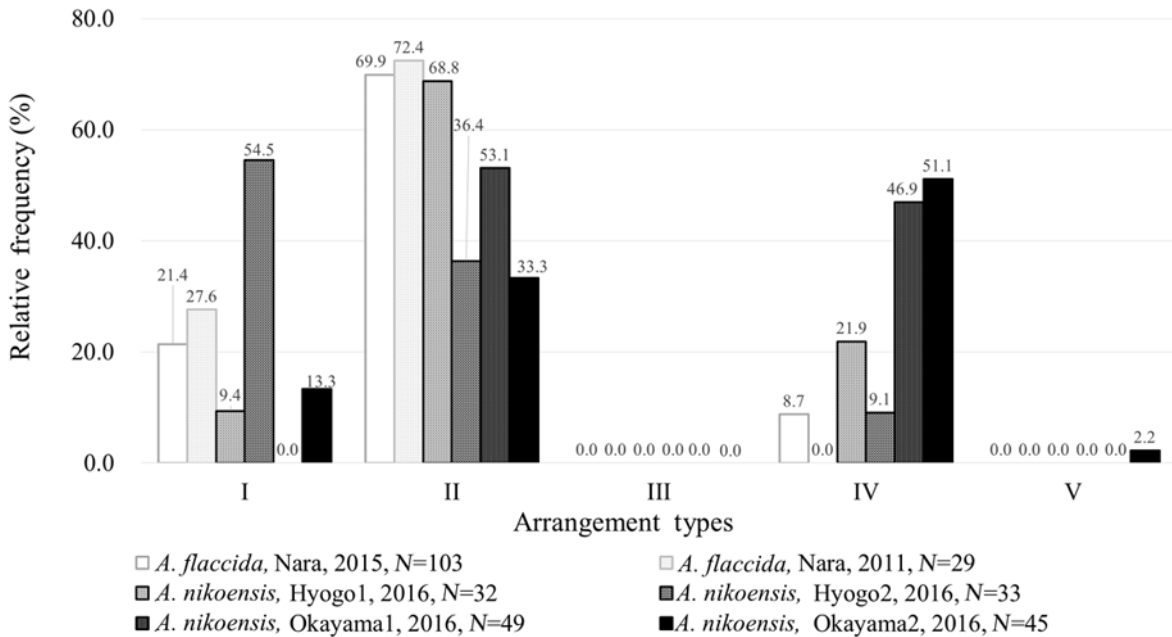


Fig. 3 Occurrence of tepal arrangements measured for flowers with six tepals in *Anemone flaccida* and *Anemone nikoensis* populations.

follow a continuous spiral arrangement with $\varphi < 144^\circ$ (Fig. 1e), with the sixth primordium located between first and third primordia in the spiral (Fig. 1d, II). In wild populations of *A. scabiosa*, *A. flaccida*, and *A. nikoensis*, the sixth tepal was selectively observed at Positions I, II, and IV with higher frequency than at Positions III and V (Fig. 2 and Fig. 3). Because angular vacancies (Eq. 2) for Types I, II, and IV are equal to Δ_2 while those for Types III and V are equal to Δ_3 , our results suggest $\Delta_2 > \Delta_3$, thus $\varphi < 144^\circ$ (Fig. 1e) in *Anemone*. This is consistent with the well-known, golden divergence angle of 137.5° in spiral phyllotaxis. Thus, constrained variation among Types I, II, and IV indicates the spiral nature of floral phyllotaxis, whereas the perfect penta-radial symmetry $\varphi = 144^\circ$ results in equal angular vacancies $\Delta_2 = \Delta_3$, and thus equal appearance of all five types.

Organ growth rate can bias toward trimerous whorls

If the angular vacancy calculated above is the whole story, the frequency must be almost equal among these three positions. However, clear preferences were found in a form-dependent manner in *A. scabiosa* (Fig. 2) and in a species-dependent manner in *A. flaccida* and *A. nikoensis* (Fig. 3). To understand the biased occurrence of the three positions, we compared the potential energy (Eq. 3) of the five arrangement types (I–V) (Fig. 4, Tab. 1). The global minimum position of the potential energy depended on φ and the sign of α . When $\alpha = 0$ (i.e., inhibition from the five organs is equal) two local minima have the same energy levels (Fig. 4a,b, black solid arrowheads) corresponding to the largest angular vacancy, with positions of the sixth organ in Types I, II ($\varphi < 144^\circ$; Fig. 1e) or III, V ($\varphi > 144^\circ$; Fig. 1f). When $\varphi < 144^\circ$ and $\alpha > 0$ (Region II in Fig. 4c), the global minimum is between the third and first organs as the position of sixth organ in Type II (Fig. 4a, grey solid line), which accounts for the highest frequency observed in *A. scabiosa* (white), *A. flaccida*, and *A. nikoensis* (Tab. 1, first

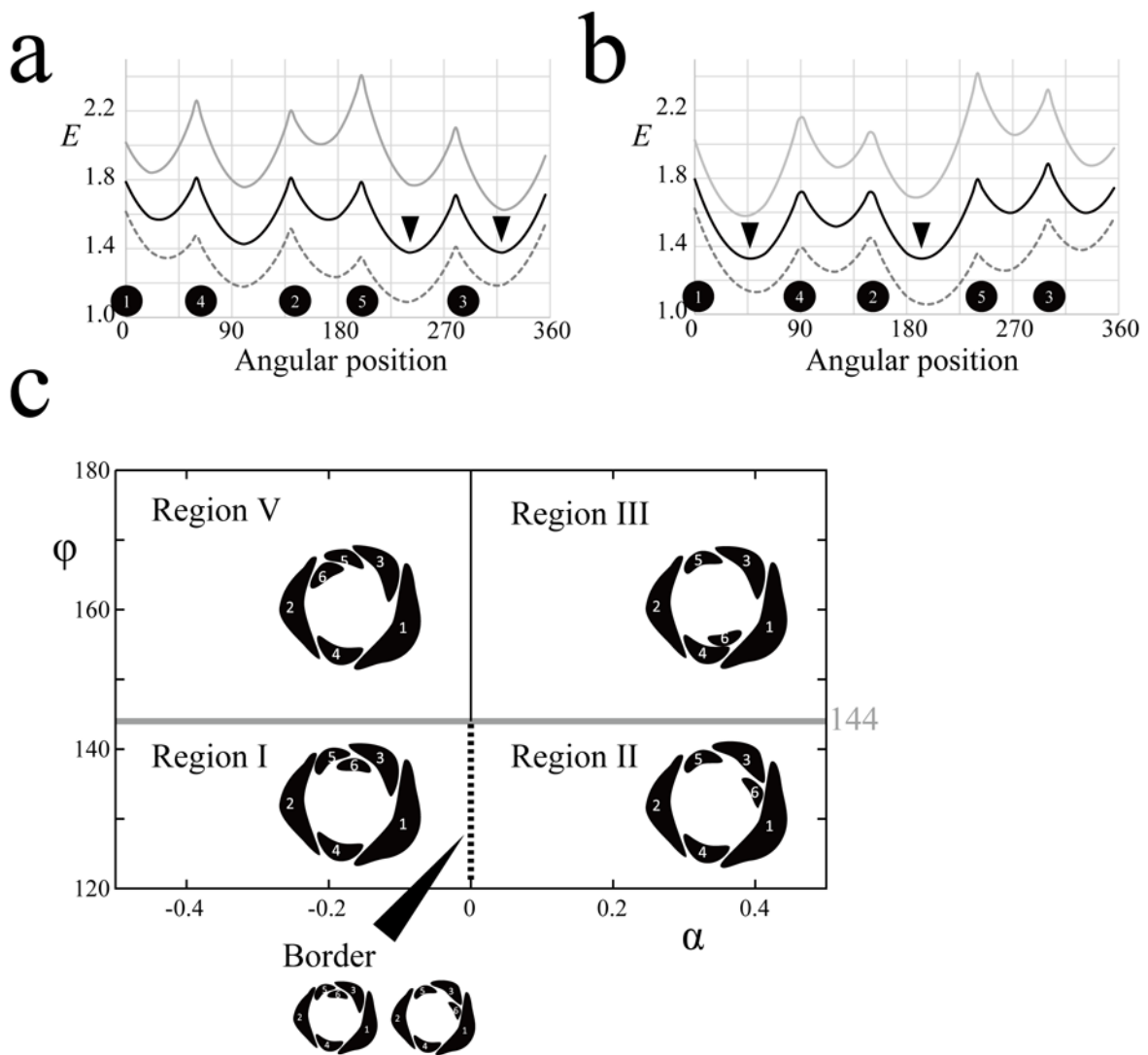


Fig. 4 Potential landscape and phase diagram of phyllotaxis model. **a** and **b** show the potential landscape representing inhibition strength on the sixth organ initiation from pre-existing organs (Eq. 3). Close circles indicate the position of five organs (Eq. 1), whose numbers correspond to those in Fig. 1e,f. Organ growth rate $\alpha = 0$ (black solid line), 0.1 (grey solid line), -0.1 (grey dashed line), and spatial-decaying length of inhibition divided by distance from centre $\lambda / R_0 = 0.5$. Divergence angle $\varphi = 140^\circ$ (**a**), $\varphi = 150^\circ$ (**b**). **d** Phase diagram indicating the most frequent arrangement types which was determined from the position taking the global minimum of potential energy. Equal frequency of Types I and II occurs only at the border $\alpha = 0$ and $\varphi < 144^\circ$.

Tab. 1 Comparison of field work of mature flowers and floral phyllotaxis model. The rank of frequency at first, second, and third are shown for *Anemone* species (sum of observed populations in Fig. 2 and Fig. 3) and model parameter regions. The position of energy minimum ranked as second switched from IV to II in Region I (from IV to I in Region II) as φ got closer to 120° .

	Rank of frequency		
	1	2	3
<i>A. scabiosa</i> (p)	IV	II	I
<i>A. scabiosa</i> (w)	II	IV	I
<i>A. nikoensis</i>	II	IV	I
<i>A. flaccida</i>	II	I	IV
Model (Region II)	II	IV/I	I/IV
Model (Region I)	I	IV/II	II/IV

rank of frequency). At the same time, the second and third local minima are located between the second and fourth organs (Type IV), and between the third and fifth organs (Type I) (Fig. 4a, grey solid line). Energy levels of the two local minima depend on φ . At a small φ close to 120° , the energy level of Type I is lower than that of Type IV, which accounts for Type I having a higher frequency than Type IV in *A. flaccida* (Tab. 1, second and third rank of frequency). At large φ up to 144° , the magnitude relation switches, which accounts for the rank of frequency in *A. scabiosa* (white) and *A. nikoensis*. Conversely, when $\varphi < 144^\circ$ and $\alpha < 0$ (Region I in Fig. 4c), the global minimum corresponded to Type I, and the second and third local minima corresponded to Types IV and II (Fig. 4a, grey dashed line). Therefore, when $\varphi < 144^\circ$ the model explains that the organ growth rate α switches the highest frequency between Types I and II while the divergence angle φ selects the second and third highest frequency among I, II, or IV. By ranking the energy levels of local minima, we estimate two developmental parameter regions: (i) $\alpha < 0$ and small φ close to 120° for *A. flaccida*, and (ii) $\alpha < 0$ and large φ up to 144° for *A. scabiosa* (white) and *A. nikoensis*.

Developmental parameters for *A. scabiosa* (pale pink) were not found in the present model (Tab. 1).

Discussion

Field work on intraspecific variation in tepal arrangement of pentamerous *Anemone* flowers (Fig. 1c) provided two primary results: (i) restriction to three types including trimerous arrangement (Fig. 1d, II) among five possibilities (Fig. 2 and Fig. 3), and (ii) species-dependent frequency bias among the three types (Tab. 1). Restriction to three arrangement types is consistent with a phyllotaxis model for sixth organ initiation with the condition being the divergence angle $\varphi < 144^\circ$. This spiral nature, rather than perfect penta-radial symmetry $\varphi = 144^\circ$, underlies the restricted occurrence of three arrangement types.

To date, parameters of meristem growth and size have been mainly focused on as a central factor controlling divergence angle φ , which mainly characterizes spiral phyllotaxis. Interestingly, for species-dependent bias, the present phyllotaxis model suggests that a factor relating to primordial growth (α) plays a major role in selecting the highest frequency type, independent of meristem growth. We found that the trimerous arrangement (Type II) is the most frequent when the older primordia have a weaker inhibitory effect ($\alpha > 0$ in Fig. 4c). The growth rate of organ primordia may bias transitions from pentamerous to trimerous whorls.

Future problems to consider for the mathematical model include the experimental validations. Our suggestion that $\varphi < 144^\circ$ can be directly validated experimentally in floral development. For example, the angle between the second and third tepal primordia seems consistently lower than 144° in *Anemone* (Figs. 7A–D and 9B in [6]). Since trimery appeared at a positive α in the present model, older organs have smaller effect on the new primordia, consistent with the observation that size differences between the first and subsequent tepal primordia were smaller in trimerous species than in pentamerous *Anemone* species (e.g., Figs. 7A–E and 13A–E in [6]). Furthermore, we need to examine the robustness of two assumptions of the present model, the constant divergence angle φ and constant rate of primordial growth α . The angle φ can differ among primordia in pentamerous flowers, since the angle between the first and second organs seems higher than 144° in *Anemone* (Figs. 7A–D and 9B in [6]). The primordial growth rate α can also be heterogeneous, as we often observed morphologically distinct tepals of a single flower (small, ovate, hairy, two outer tepals

and large, obovate, three inner tepals) in pentamerous *A. scabiosa*. For model robustness, it is interesting to examine the effect of the observed primordia-dependent heterogeneity of ϕ and α on biased occurrence of the arrangements.

Another avenue for future research is extensive field work on other genera and families as well as other *Anemone* species to determine whether constrained variation between pentamerous and trimerous is common and symmetric. For example, in trimerous flowers showing intraspecific variation including reduced tepal number (e.g., *Anemone nemorosa* [19], *Eranthis hyemalis* (Ranunculaceae) [20], and the genus *Magnolia* (Magnoliids) [21]), we can identify which tepal is stochastically lost in the same manner as the present study (Fig. 1c,d). This information would clarify whether trimerous whorls selectively transition to quincuncial pentamery (Fig. 1c) or other arrangements. Similarly, field observations and a floral phyllotaxis model can be designed to examine phenotypic variation with more than six perianth organs. Such a study would elucidate whether Types I and IV (Fig. 1d) are merely obstacles of transition to trimerous whorls (Type II), or actual transient states to other novel arrangements such as the perianth double whorl (Fig. 1a), which may cause inter-specific difference.

References

1. Endress PK. The flowers in extant basal angiosperms and inferences on ancestral flowers. *Int J Plant Sci.* 2001;162(5):1111–1140. <https://doi.org/10.1086/321919>
2. Douady S, Couder Y. Phyllotaxis as a dynamical self organizing process Part II: the spontaneous formation of a periodicity and the coexistence of spiral and whorled patterns. *J Theor Biol.* 1996;178(3):275–294. <https://doi.org/10.1006/jtbi.1996.0025>
3. Smith RS, Guyomarç'h S, Mandel T, Reinhardt D, Kuhlemeier C, Prusinkiewicz P. A plausible model of phyllotaxis. *Proc Natl Acad Sci USA.* 2006;103(5):1301–1306. <https://doi.org/10.1073/pnas.0510457103>
4. Kitazawa MS, Fujimoto K. A dynamical phyllotaxis model to determine floral organ number. *PLoS Comput Biol.* 2015;11(5):e1004145. <https://doi.org/10.1371/journal.pcbi.1004145>
5. Hoot SB, Meyer KM, Manning JC. Phylogeny and reclassification of *Anemone* (Ranunculaceae), with an emphasis on austral species. *Syst Bot.* 2012;37(1):139–152. <https://doi.org/10.1600/036364412X616729>
6. Ren YI, Chang HL, Endress PK. Floral development in Anemoneae (Ranunculaceae). *Bot J Linn Soc.* 2010;162(1):77–100. <https://doi.org/10.1111/j.1095-8339.2009.01017.x>
7. Ronse De Craene L. Meristic changes in flowering plants: how flowers play with numbers. *Flora.* 2016;221:22–37. <https://doi.org/10.1016/j.flora.2015.08.005>
8. Kitazawa MS, Fujimoto K. A developmental basis for stochasticity in floral organ numbers. *Front Plant Sci.* 2014;5:545. <https://doi.org/10.3389/fpls.2014.00545>
9. Kitazawa MS, Fujimoto K. Relationship between the species-representative phenotype and intraspecific variation in Ranunculaceae floral organ and Asteraceae flower numbers. *Ann Bot.* 2016;117(5):925–935. <https://doi.org/10.1093/aob/mcw034>
10. Adler I. A history of the study of phyllotaxis. *Ann Bot.* 1997;80(3):231–244. <https://doi.org/10.1006/anbo.1997.0422>
11. Cunnell GJ. Aestivation in *Ranunculus repens* L. *New Phytol.* 1958;57(3):340–352. <https://doi.org/10.1111/j.1469-8137.1958.tb05323.x>
12. Zhao L, Bachelier JB, Chang HL, Tian XH, Ren Y. Inflorescence and floral development in *Ranunculus* and three allied genera in Ranunculeae (Ranunculoideae, Ranunculaceae). *Plant Syst Evol.* 2012;298(6):1057–1071. <https://doi.org/10.1007/s00606-012-0616-6>
13. Gonçalves B, Nougé O, Jabbour F, Ridet C, Morin H, Laufs P, et al. An *APETALA3* homolog controls both petal identity and floral meristem patterning in *Nigella damascena* L. (Ranunculaceae). *Plant J.* 2013;76(2):223–235. <https://doi.org/10.1111/tpj.12284>
14. Wang P, Liao H, Zhang W, Yu X, Zhang R, Shan H, et al. Flexibility in the structure

- of spiral flowers and its underlying mechanisms. *Nat Plants*. 2015;2:15188. <https://doi.org/10.1038/nplants.2015.188>
15. Coen ES, Meyerowitz EM. The war of the whorls: genetic interactions controlling flower development. *Nature*. 1991;353(6339):31–37. <https://doi.org/10.1038/353031a0>
 16. Douady S, Couder Y. Phyllotaxis as a dynamical self organizing process Part I: the spiral modes resulting from time-periodic iterations. *J Theor Biol*. 1996;178(3):255–273. <https://doi.org/10.1006/jtbi.1996.0024>
 17. Mirabet V, Besnard F, Vernoux T, Boudaoud A. Noise and robustness in phyllotaxis. *PLoS Comput Biol*. 2012;8(2):e1002389. <https://doi.org/10.1371/journal.pcbi.1002389>
 18. Refahi Y, Brunoud G, Farcot E, Jean-Marie A, Pulkkinen M, Vernoux T, et al. A stochastic multicellular model identifies biological watermarks from disorders in self-organized patterns of phyllotaxis. *eLife*. 2016;5:e14093. <https://doi.org/10.7554/eLife.14093>
 19. Yule GU. Variation of the number of sepals in *Anemone nemorosa*. *Biometrika*. 1902;1(3):307–308. <https://doi.org/10.1093/biomet/1.3.307>
 20. Salisbury EJ. Variation in *Eranthis hyemalis*, *Ficaria verna*, and other members of the Ranunculaceae, with special reference to trimery and the origin of the perianth. *Ann Bot*. 1919;os-33(1):47–79.
 21. Zagórska-Marek B. Magnolia flower – the living crystal. *Magnolia*. 2011;89:11–21.